Exploring the Dynamics of TCR-pMHC Interactions: A Computational Analysis of Nanoparticle Binding and T Cell Activation

Huilin Tai

April 10, 2024

Abstract

Our interest lies in exploring how the binding rate is influenced by the diversity of T cell receptor (TCR) distributions. Therefore, we have designed nanoparticles that exhibit efficient binding to TCRs with uniform distribution while showing minimal interaction with clustered TCRs. Concurrently, we are examining whether nanoparticles exist that demonstrate more effective binding to clustered TCRs compared to those uniformly distributed on the cell surface.

In the context of potential therapeutic applications for autoimmune diseases, nanoparticles (NPs) layered with peptide-major histocompatibility complexes (pMHCs) are emerging as promising tools for the reprogramming of specific CD4+ T cells into disease-alleviating T regulatory type 1 (Tr1) cells. This reprogramming process is made possible by NPs binding to T cell receptors (TCRs) presented in the form of TCR nanoclusters (TCRnc). The effectiveness of such therapy can be modulated by altering both the size of the NPs and the quantity of pMHCs layered onto them, a characteristic known as valence. The multilevel binding process involving TCR-pMHC, NP-TCRnc, and T cell is therefore polyvalent. This study delves into the principles governing the design of multivalent nanoparticles, aiming to advance their use in T-Cell therapy. By modelling the binding dynamics between T cells and nanoparticles, we strive to identify the critical geometric properties of NP-TCR interactions that drive selective binding and to understand their contribution to this process.

1 Introduction

As we assume tcr are distributed in poisson distribution on suffice of cell, and tcr clusters are also poisson distributed on the surface. we use math model to simulate and visualize the distribution. the binding probability is

After binding to TCRs, pMHC-coated NPs form aggregates on the surface of T cells. Recent studies have shown that TCRs, known as TCR nanoclusters (TCRnc),are organized even before stimulation[1]. These TCRnc contain up to 20 TCRs, distributed over regions of radius up to 200 nm, and are crucial for proper T cell activation. The geometrical properties of TCRnc provide a framework to understand the polyvalent binding of pMHC-NPs with TCRnc. The spatial distribution of TCR on the surface of T cells is constrained by the arrangement of TCR into TCRnc complexes, which requires a minimum distance between two TCRs due to the co-receptors associated with each of these

TCRs occupying a region that cannot be occupied by any other. Polyvalent presentation of ligands or receptors can significantly increase ligand-receptor binding through mechanisms such as chemical cooperativity or mechanistic effects. Investigating the impact of geometry on T cell activation, commonly assessed through interferon-γ (IFNγ) release, has the potential to enhance the design of nanoparticles (NPs) to promote Tr1-cell response, while also shedding light on the underlying dynamics of TCR-pMHC interactions. In this research, we utilize both computational and modeling approaches to conduct a comprehensive analysis. While serial engagement may be specific to immune synapses, it is very plausible that this mechanism of interaction also occurs between T cells and the pMHC-coated NPs in a polyvalent manner. It has been suggested that in the context of an immune synapse, pMHCs can serially engage 200 TCRs [4,5]. Hence further implementation of the serial engagement mode, which links T cell activation to the interaction duration between the receptor (TCR) and ligand (pMHC) was conducted to investigate whether our multi-scale model can trigger jumps between IFNγ dose-response curves produced by T cells following NP stimulation when the valence of pMHC (total number of pMHCs on NPs), denoted by v, is modestly altered for a given NP size. Our objective is to ascertain whether the interaction geometry can facilitate T-cell activation.

2 Modeling

Researchers from the University of Calgary's Santamaria Lab examined the effects of NP design on T cell activation by exposing 25,000 CD8+ T cells to rigid and non-deformable gold NPs coated with cognate pMHCs at varying concentrations, radii, and valences. T cell response data in terms of interferonγ (IFNγ) secretion was collected, after incubating the cells for 48 hours. The present study employs a serial engagement model to investigate T-cell binding to nanoparticles (NPs) while incorporating the relevant geometries associated with this interaction at various scales[2]. These scales encompass the contact area level, which involves the T cell receptor (TCR)-peptide-major histocompatibility complex (pMHC) binding, the TCR nanocluster level, which refers to the nanoscale structures formed by TCRs on the membrane of T cells, and the T cell level.

Contact Area Model (CAM) imposes geometric constraints on the polyvalent interaction between a clustered set of TCRs and a NP. Restricted number of pMHCs in the contact area is known as the effective valence, denoted $\widetilde{v}$, and is quantified using the expressions:

$$CA = 2\pi \int_{0^\circ}^{\pi/4} r^2 sin\theta d\theta = \sqrt{2}(\sqrt{2}-1)\pi r^2 \tag{1}$$

$$\widetilde{v} = v\frac{CA}{SA} = v\frac{\sqrt{2}(\sqrt{2}-1)\pi r^2}{4\pi r^2} \approx v/7 \tag{2}$$

The contact area angle θ defines the region of interaction between the NP and T cell, limiting the number of available surface pMHCs for binding. The number of TCRs in the contact area is constrained by TCR density, which is determined by the minimum distance between TCRs (dTCR), the radius of TCR nanoclusters (rnc) and the number of TCRs per nanocluster (nTCR). By projecting the contact area onto the T cell surface, we can estimate the number of available TCRs. By letting X_i = Proportion of NPs with i bound TCRs, we can design a Markov model in which the transitions between these states represent pMHC-TCR binding and unbinding events with dynamic of this model

given by:

$$N = \min(N_T, \tilde{v}). \tag{3}$$

for $i = 1, \ldots, N$

$$\frac{dX_i}{dt} = k_{on} P_{i-1} \tilde{v}(N_T - i + 1) X_{i-1} - (k_{on} P_i \tilde{v}(N_T - i) + k_{off}) X_i + (i+1) k_{off} X_{i+1} \tag{4}$$

The average dwell time $\hat{\tau}(N)$ before a NP completely detaches from the TCR_{nc} can be expressed as

$$\hat{\tau}(N) = \sum_{i=0}^{N} \hat{X}_i \tau_i = \langle \hat{\mathbf{X}}, \boldsymbol{\tau} \rangle, \tag{5}$$

where $\hat{\mathbf{X}} = (\hat{X}_0, \hat{X}_1, \ldots, \hat{X}_N)$.

TNM can be also used to compute the insertion probabilities associated with NP binding to a $\mathrm{TCR}_{\mathrm{nc}}$, while additionally providing estimates for M, the theoretical maximum carrying capacity of a $\mathrm{TCR}_{\mathrm{nc}}$. The distribution of TCRs covered by a NP, ρ_ι can be determined using the expression

$$\rho_\iota(n) \approx \frac{\text{Number of simulated } \iota^{\text{th}} \text{ NP covering } n \text{ TCRs}}{\text{Total number of simulated } \iota^{\text{th}} \text{ NP}}.$$

And a probability estimate for the ability of a $\mathrm{TCR}_{\mathrm{nc}}$ to bind at least j NPs or more is calculated as follows

$$q(j) \approx \frac{\text{Number of simulated TCR}_{\mathrm{nc}} \text{ such that } c_{NP} \geq j}{\text{Total number of simulated TCR}_{\mathrm{nc}}}.$$

The Markov Model's transition rates include insertion probabilities, which are estimated by Monte Carlo simulations of the contact area geometry. For a given configuration where i pMHC-TCR bonds have formed, the corresponding P_i denotes the fraction of available pMHCs for subsequent binding. These probabilities account for steric effects of ligand-receptor binding as each pMHC-TCR bond limits further binding in a 10 nm diameter region. After random pMHC configurations and initial TCR binding are set, TCR positions are adjusted to ensure sufficient separation. The insertion probabilities are then calculated from the remaining pMHCs available for binding, assuming immobile TCRs and relocating TCR positions for statistical estimates[7].

With TAM model, once the number of triggered TCRs per T cell is determined, the actual quantity of IFNγ produced, denoted by $y(x)$ (where x is the number of triggered TCRs), is calculated using the expression

$$\log(y(x)) = \max\{\log(15), \mu \cdot (1 - \exp(-A(x - C))\}, \tag{6}$$

where μ is the maximum level of activation, A is the rate of activation increase and C is the activation threshold. The log(15) term accounts for the basal level of IFNγ release by a T cell. This expression mimics the profile of IFNγ release from a T cell obtained upon stimulation with a peptide, antigen or CD3 as a function of triggered TCRs.

In order to prepare the multi-scale model for subsequent analyses, we quantified the insertion probabilities of pMHCs and NPs in the CAM and TNM models[2]. We also determined the dwell-time NPs spent bound to TCRnc as a function of the dissociation constant and computed the distributions of covered and bound TCRs per NP for NP sizes of r = 14nm. Further, by combining the CAM with TNM dynamics, we explored the

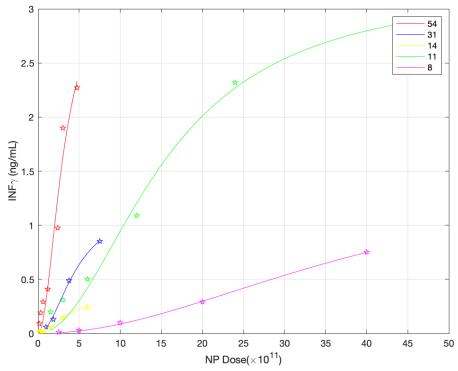

[1-a]

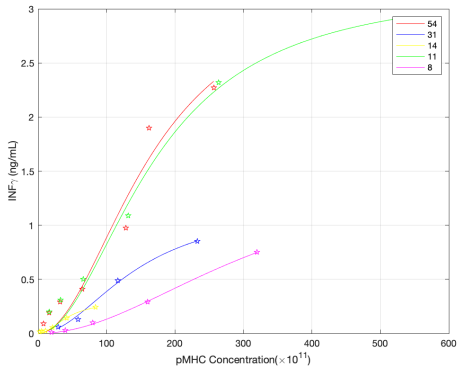

[1-b]

Figure 1: **Hill function fitting based on the experimental dose-response data, coded for pMHC density on the NP density.** IFNγ dose-response curves of simulated data with NP radius(r) = 14. Each curve corresponds to a specific valence v and is color-coded according to the legend of each panel.

performance of the model by comparing it to dose-response curves of interferon-γ (IFNγ) release from T cells upon NP stimulation. My work is based on the reverse engineering approach mentioned above to model pMHC-coated NPs binding to T cells to study developed models analytically and numerically and against experimental data through Markov Chain Monte Carlo (MCMC) techniques for polyvalent, spatially constrained ligand/receptor systems[6].

3 Results

3.1 Data Simulation

In order to investigate the non-linear "jump" observed between the two dose-response curves, a hill function constituted a small data set. An optimization process was run based on the function f(x)= $\frac{b_1*(x^n)}{b_2^n+x^n}$ to determine the best parameters for fitting each valence, where n represents the Hill coefficient, b_1 represents maximal production rate and b_2 is activation coefficient. Comparing the sum of squared error calculated by SSE=$\sum_{i=1}^{D}(f(x_i)-y_i)^2$ with n ranging between 1 to 20, the optimal degree n was found to be 2, and hence a function was generated for each valence (8, 11, 14, 31, and 54), as shown in figure[1-a]. The model plotted with respect to pMHC concentration rather than NP concentration is also shown in figure[1-b], revealing a similar pattern between curves of valence 54 and valence 11, indicating saturation in T cell response. Based on the hill function models generated, 100 data points were simulated for each valence, with NP dose ranging from 0.1 to 50 and evenly distributed across 100 numbers. Through the hill function fitting we expanded the experimental data set to 300 points of simulated data, providing more points for the following MCMC fitting. In line with the range of NP dose in the experimental data, the simulated data is a more informative and comprehensive data set, which can help fit the outcomes of the multi-scaled model to the dose-response curves.

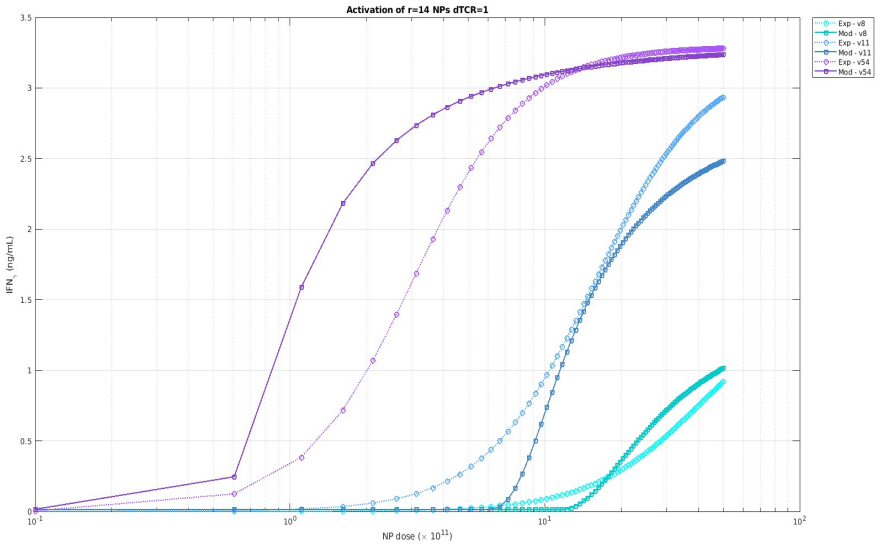

Figure 2: **IFNγ dose-response curves and model predictions with respect to NP concentration for dTCR=1nm.** Model parameters are estimated by fitting the multiscale model (solid curves) to simulated IFNγ dose-response curves (dashed curves) when r = 14 nm. Each curve corresponds to a specific valence v and is color-coded according to the legend of each panel.

3.2 Model Fitting and Model Selection

With the simulated data, we started with fitting the multi-scale model with 5 parameters:kd, $alpha$, μ, C, and KD to the Hill functions produced in the previous section, where kd is the dissociation constant of monovalent pMHC-TCR binding/unbinding rates; $alpha$ represents the activation coefficient;C is the activation threshold; μ is the parameter defining the maximum level of cellular IFNγ production; KD represents mean passage time of the NPs. In contrast to the previous affinity-centric model [2], the serial engagement model approach resulted in a significantly shorter processing time and lower least square error. Consequently, the investigation was conducted to assess the potential contribution of the serial engagement model to the pMHC-density dependent thresholds that elicit jumps in the IFNγ dose-response curve. As the model employs five parameters, the MCMC algorithm was iterated for over 500,000 times, resulting in an optimal parameter set with a least square error of 21.8. This outcome is promising given the size of the data set, which comprises 300 points. Since the least square error is considered stable and the parameters have a short burning time, we decided to cease iterating and evaluate the outcome. Upon plotting all parameters against each other, we observed some intriguing patterns between certain parameters, including a parabolic correlation between mu and alpha, a linear correlation between KD and kd, and a linear correlation between C and kd. With our parameters, the model for valence 8 and 11 showed signs of capturing the jump, which hence explains the significant increase of the maximum activation reached by each specific valence [2][3].

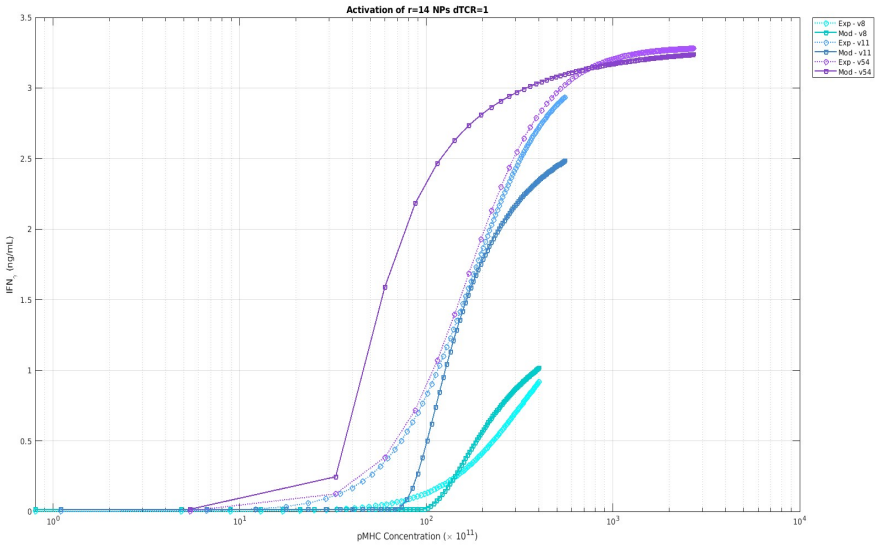

Figure 3: **IFNγ dose-response curves and model predictions with respect to pMHC concentration for dTCR=1nm.** Model parameters are estimated by fitting the multiscale model (solid curves) to simulated IFNγ dose-response curves (dashed curves) when r = 14 nm. Each curve corresponds to a specific valence v and is color-coded according to the legend of each panel.

3.3 Investigation in Probability Distribution Difference

The model above that captures the "jump" is facilitated with the value of kd smaller than 1, which means $\frac{k_{off}}{k_{on}} < 1$, indicating that pMHC and TCR are more likely to bind than unbind. To investigate the impact of the small value of kd to TCR density, a probabilistic approach was explored for further quantification, given the observed slight differences in the dwell time distribution of valence 8 and valence 11, as well as the number of serially engaged TCRs per TCRnc distribution between the two valences. It was hypothesized that these distribution differences may serve as the trigger for the observed jump. As the probability distribution is influenced by dTCR, which is the distance required between TCR and nTCR, which represents the number of TCR per nano-cluster, a comparison was made between valence 8 and valence 11 with fixed dTCR=1nm and nTCR values of 20, 50, 100, 200, and 500. The results indicate that larger nTCR values led to greater differences between the two valences in both dwell time distribution and the number of serially engaged TCRs per TCRnc distribution, while the difference in the latter distribution between the 2 valences is more significant. Given that nTCR values in realistic settings may not be identical between valence 8 and valence 11, it was of interest to determine the degree of difference in nTCR required to produce a significant difference in the distribution of dwell time and serially engaged number. Several pairs of nTCR for valence 8 and 11 were tested, including (10,20), (20,50), (20,100), (100,200) and (100,500). The overlap between the probability distributions of valence 8 and valence 11 were calculated, when nTCR for valence 8 was 100 and nTCR for valence 11 was 500 the overlap is approximately 20%, however, the pair of (20,200) resulted in an overlap of approximately 50%. As shown in figure[4] and figure[5], the gap between nTCR of valence 8 and 11 has to be considerable to generate significantly different distribution.

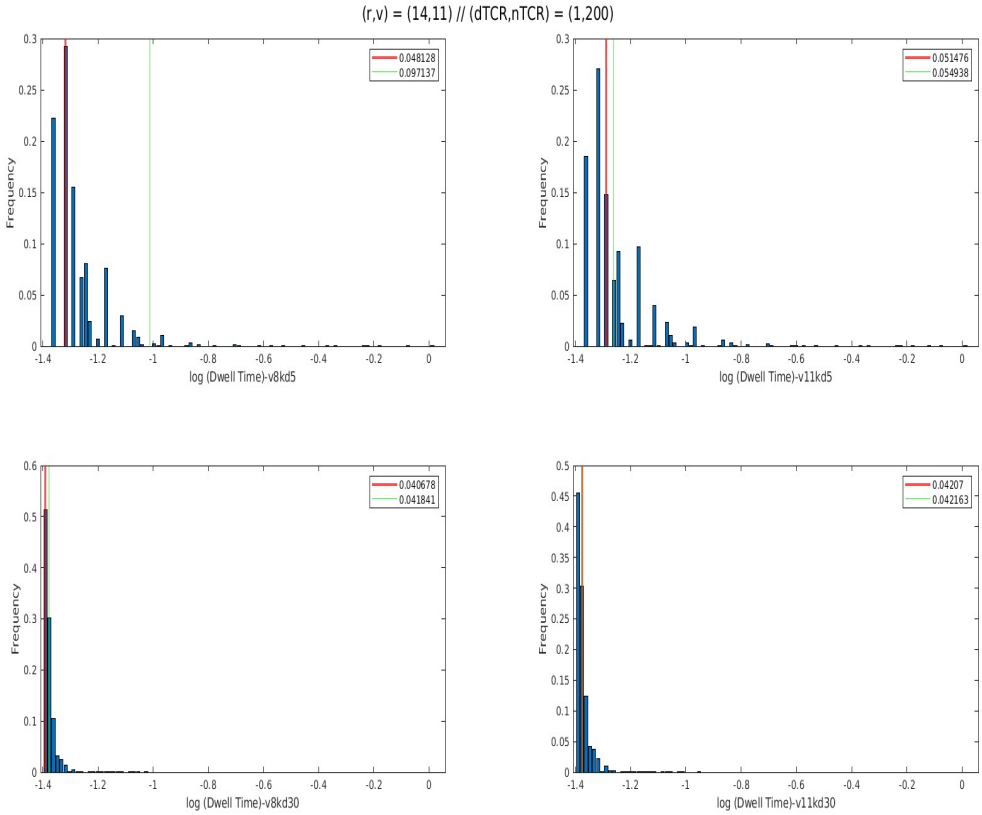

Figure 4: **Probability distribution contrast for number of serially engaged TCRs per TCRnc and dwell time with kd=5 and kd=30.** The mean of distribution (green line) and median value of distribution (red line) are generated. Distributions vary depending on the dissociation constant of monovalent pMHC-TCR binding/unbinding rates for valence 8 and 11.

3.4 Modified Model with Probability Distribution Difference

Though the jump was captured by previous model, we can see the model fitting was not ideal with respect to shape and starting point of T cell activation. To improve the model and investigate the contribution of probability distribution to T cell activation, a new parameter multiplier was added as a parameter to the initial model, which consisted of kd, $alpha$, C, mu, and KD parameters. Multiplier $= \frac{nTCR_{v11}}{nTCR_{v8}}$, where nTCR_{v8} represents nTCR of valence 8, nTCR_{v11} is nTCR for valence 11. We started with setting nTCR_{v8} to be 20, and used rounded Multiplier$*\text{nTCR}_{v8}$ as nTCR_{v11}. Through this approach, our model takes probability distribution into account because valence 8 and 11 have different TCR densities, leading to varying insertion probabilities due to their different nTCR. However, with 6 parameters and different insertion probability every iteration, we found it hard to achieve a good fitting in acceptable polynomial running time.

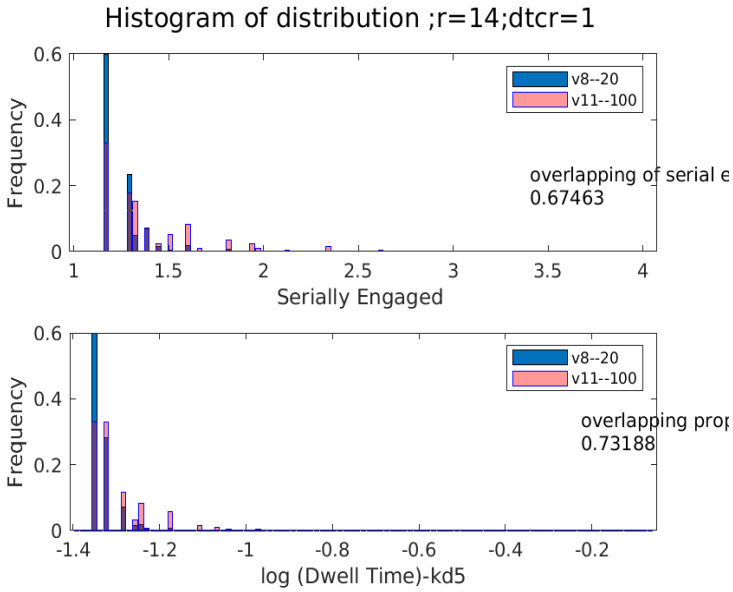

Figure 5: **Probability distribution overlap of number of serially engaged TCRs per TCRnc and dwell time for (20,100).** The distribution for valence 8 when dtcr=20 is in blue, while distribution for valence 11 when dtcr=100 is in pink, overlapping proportion is calculated.

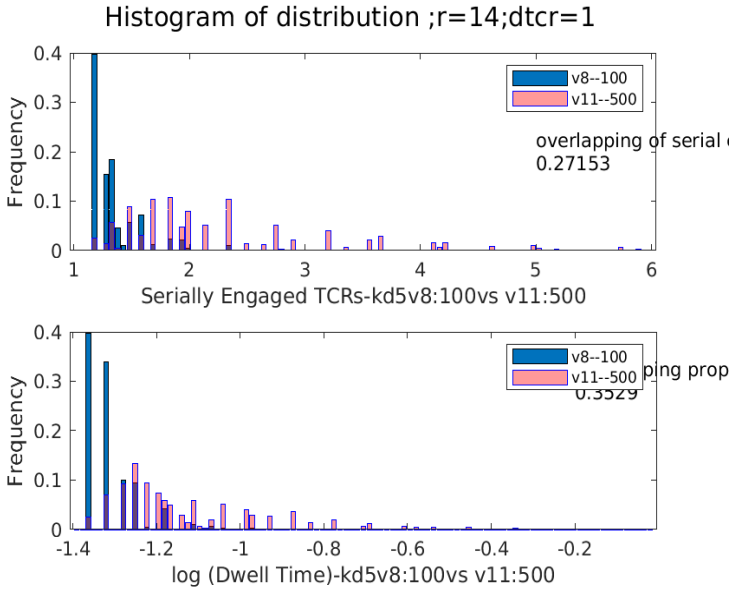

Figure 6: **Probability distribution overlap of number of serially engaged TCRs per TCRnc and dwell time for (100,500).** The distribution for valence 8 when dtcr=100 is in blue, while distribution for valence 11 when dtcr=500 is in pink, overlapping proportion is calculated.

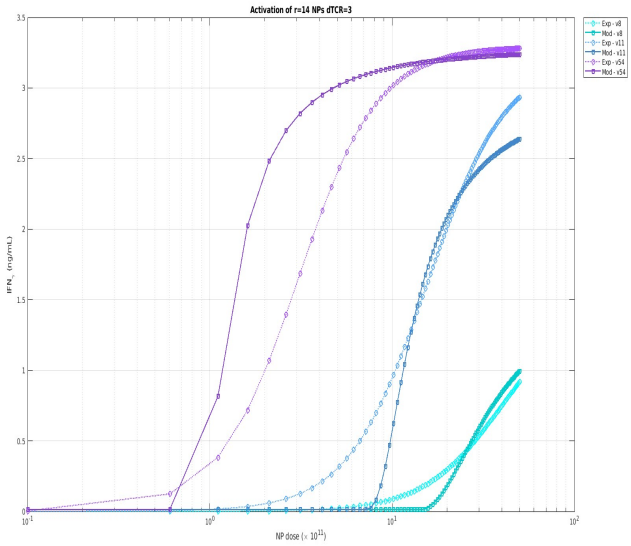

Figure 7: **IFNγ dose-response curves and model predictions with respect to NP concentration for dTCR=3nm.** Model parameters are estimated by fitting the multiscale model (solid curves) to simulated IFNγ dose-response curves (dashed curves) when r = 14 nm. Each curve corresponds to a specific valence v and is color-coded according to the legend of each panel.

4 Discussion and Conclusion

In this study, we modeled the polyvalent binding of NPs to T cells based on the geometrical properties of this system. Based on the developed serial engagement model[2] of T cell binding to NPs and incorporated the relevant geometries associated with this interaction at the contact area level, the TCR nanocluster level, and the T cell level, we found that the sensitivity of T-cell activation to NP valence can be explained by the geometric properties of TCR/pMHC binding. Simulated data was applied to MCMC in order to estimate model parameters, yielding a significant improvement to the quality of the fits compared with conducting fitting with experimental data directly. With kd, the dissociation constant of monovalent pMHC-TCR binding/unbinding rate smaller than 1, our model was able to capture the jump in T-cell activation when switching between NP incapable and capable of polyvalent binding between $v = 8$ and $v = 11$ for the 14 nm NP, proving geometric constraints are responsible for the dynamics of dynamics of TCR/NP binding and the viability of serial engagement model.

For the model that captured the jump we mentioned above, dTCR was fixed to be 1. Since IFNγ production is determined directly from the number of bound TCRs, future exploration is needed to see if specific pattern of the distance between TCR (dTCR) is required to capture the jump in T-cell activation when switching between NP incapable and capable of polyvalent binding (e.g. between $v = 8$ and $v = 11$ for the 14 nm NP). For dTCR=3, we found that it is also capable of explaining valence sensitivity and capturing the jump(seen in figure[7][8]). Further explorition could be conducted to check model robustness for larger dTCR. Also, several correlation patterns were observed between parameters in our parameter chain of 45000 iterations, which require further validation on the scale of total iteration numbers to decide if the correlation is global. If so, it is

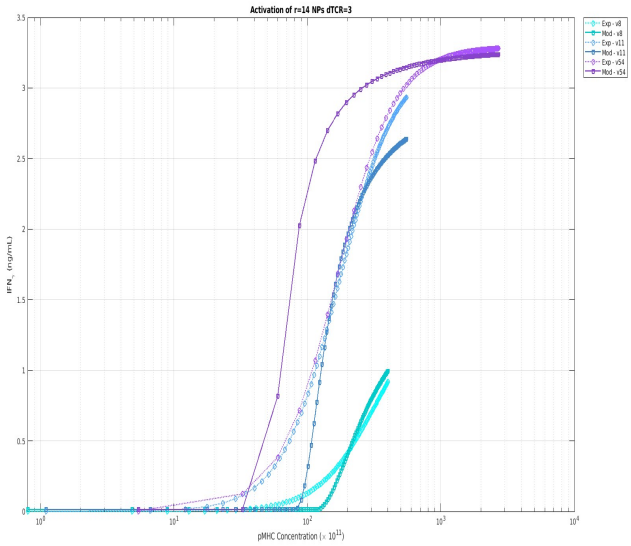

Figure 8: **IFNγ dose-response curves and model predictions with respect to pMHC concentration for dTCR=3nm.** Model parameters are estimated by fitting the multiscale model (solid curves) to simulated IFNγ dose-response curves (dashed curves) when r = 14 nm. Each curve corresponds to a specific valence v and is color-coded according to the legend of each panel.

also possible to simplify the model structure by merging parameters for improvement. We noticed a small value of parameter kd played an important role of reproducing the jump in our model which is based on serial engagement model, it is also worth investigating if similar pattern of parameter kd applied to model based on the affinity-centric model would also be able to capture the jump.

References

[1] Kumar, R. Ferez, M. Swamy, M. et al. 2011. Increased sensitivity of antigen-experienced T cells through the enrichment of oligomeric T cell receptor complexes. Immunity 35:375.

[2] Pineros-Rodriguez M, Richez L, Khadra A. Theoretical quantification of the polyvalent binding of nanoparticles coated with peptide-major histocompatibility complex to T cell receptor-nanoclusters. Math Biosci. 2023 Apr;358:108995. doi: 10.1016/j.mbs.2023.108995. Epub 2023 Mar 15. PMID: 36924879.

[3] Salvatore Valitutti, Sabina Muller, Marina Cella, Elisabetta Padovan, and Antonio Lanzavecchia. Serial triggering of many T-cell receptors by a few peptide-MHC complexes. Nature, 375(6527):148–151, 1995.

[4] Wofsy, C. Coombs, D. and Goldstein, B. 2001. Calculations show substantial serial engagement of T cell receptors. Biophysical journal 80:606.

[5] Dushek, O. Aleksic, M. Wheeler, R. J. et al. 2011. Antigen potency and maximal efficacy reveal a mechanism of efficient T cell activation. Science signaling 4:ra39.

[6] Shang Wang Liu. Mathematical modelling of biophysical dynamics of nanoparticle interaction with T cells. Master's thesis, McGill University, 2015.

[7] Pineros-Rodriguez, M. 2018. Biophysics of nano-Vaccines in relation to autoimmunity McGill University (Canada).